[PCCP

ARTICLE TYPE

Cite this: DOI: 00.0000/xxxxxxxxxx

Supplementary information of Stark effect and orbitals hybridization of moiré interlayer excitons in the $MoSe_2/WSe_2$ heterobilayer.

Houssem Eddine Hannachi[a] and Sihem Jaziri [a,b]

Received Date
Accepted Date

DOI: 00.0000/xxxxxxxxxx

Contents

1 Methods of Resolution

The studied moiré interlayer exciton with an applied electric field can be described by the envelop Schrödinger equation in the effective mass approximation as follows:

$$\hat{H}_{ix}\Psi^{n,\ell}_{J,L}(r,\theta,R,\Phi) = E^{n,\ell}_{J,L}(\Delta F_{\perp(//)})\Psi^{n,\ell}_{J,L}(r,\theta,R,\Phi). \tag{1}$$

Here, the eigenvalue $E^{n,\ell}_{J,L}(\Delta F_{\perp(//)})$ defines the total energy, which can be determined by direct diagonalization of $\hat{H}_{ix}(\Delta F_{\perp(//)})$ into the basis $\Psi^{n,\ell}_{J,L}(r,\theta,R,\Phi) = \phi_{n,\ell}(r,\theta)\times\Xi_{J,L}(R,\Phi)$. Here, $\phi_{n,\ell}(r,\theta)$ and $\Xi_{J,L}(R,\Phi)$ are the solutions of the internal and center-of-mass motion problems, respectively. The eigenstate $\phi_{n,\ell}(r,\theta)$ adequately corresponds to the 2D hydrogen wavefunction in polar coordinates as[2]:

$$\phi_{n,\ell}(r,\theta) = \frac{R_{n,\ell}(r)}{a_B\sqrt{2\pi}}e^{i\ell\theta}. \tag{2}$$

Here, n and ℓ represent the principal quantum number and the angular momentum, respectively. For $n = 1,2,3,...$ and $-(n-1)\leq\ell\leq(n-1)$, the states are $(2n-1)$ fold degenerate, labeled as s for $\ell=0$, p for $\ell=\pm1$, and d for $\ell=\pm2$. The radial part is expressed in terms of Laguerre polynomials as: $R_{n,\ell}(r) = C_{n,\ell}e^{-\frac{r\alpha_n}{2a_B}}(\alpha_n\frac{r}{a_B})^{|\ell|}L^{2|\ell|}_{n-|\ell|-1}(\alpha_n\frac{r}{a_B})$. Here, $C_{n,\ell} = \frac{4}{(2n-1)^{\frac{3}{2}}}\left(\frac{(n-|\ell|-1)!}{(n+|\ell|-1)!}\right)^{\frac{1}{2}}$ is the normalization constant and $\alpha_n = \frac{4}{2n-1}$.

On the other hand, the center-of-mass eigenstate $\Xi_{J,L}(R,\Phi)$ is given by the 2D harmonic oscillator basis, which is expressed in polar symmetry as[1,2]:

$$\Xi_{J,L}(R,\Phi) = \frac{e^{iL\Phi}}{\sqrt{2\pi\Lambda_{J,L}}}Y_{J,L}(R). \tag{3}$$

Here, J and L $(-J\leq L\leq J)$ represent the principal quantum number and the angular momentum, respectively. Careful consideration is necessary in the choice of L, where $J-|L|$ must be an even number, and the total state degeneracy will be $J+1$. $\Lambda_{J,L} = \frac{R_c^2}{2}(\frac{J-|L|}{2}+1)_{|L|}$

[a] Laboratoire de Physique des Matériaux, Faculté des Sciences de Bizerte, Université de Carthage, 7021 Zarzouna, Tunisie; E-mail: hannachi.houssemedine@fsb.ucar.tn
[b] Laboratoire de Physique de la Matière Condensée, Faculté des Sciences de Tunis, Université de Tunis El Manar, 2092 El Manar, Tunisie; E-mail: sihem.jaziri@fsb.rnu.tn

is a normalization factor, and $(x)_n = \frac{\Gamma(x+n)}{\Gamma(x)}$ is the Pochhammer symbol. The radial part $Y_{J,L}(R) = (\frac{R}{R_c})^{|L|} e^{-\frac{R^2}{2R_c^2}} L^{|L|}_{\frac{J-|L|}{2}}(R^2/R_c^2)$, with $L_a^b(x)$ being the Laguerre polynomials.

1.1 Internal Motion: Binding Energy

To accurately model the exciton binding energy under an external electric field, we numerically solve the Mott-Wannier exciton equation:

$$\hat{H}_{IM}\phi_{n,\ell}(r,\theta) = E_{n,\ell}(\Delta F_{//(\perp)})\phi_{n,\ell}(r,\theta). \tag{4}$$

Here, the term $\hat{H}_{IM} = H_{IM} + \xi(\Delta F_{//(\perp)})$ is defined, where $E_{n,\ell}$ represents the relative energy. We define the binding energy as $E^b_{n,\ell}(\Delta F_{//(\perp)}) = -E_{n,\ell}(\Delta F_{//(\perp)})$, and their corresponding eigenvectors $|\psi_{n,\ell}\rangle = \sum_{n,|\ell|<n} C^{\tilde{n},\tilde{\ell}}_{n,\ell}(\Delta F_{//(\perp)})|\phi_{n,\ell}\rangle$ for both intralayer and interlayer excitons. Here, $C^{\tilde{n},\tilde{\ell}}_{n,\ell}$ are the dominant coefficients of the eigenvectors, which can be determined through the numerical diagonalization of equation (4). The electric field dependence of these coefficients is crucial for exploring the exciton Stark effect and orbitals hybridization.

1.2 Center-of-Mass Motion

In our model, we anticipate that the in-plane electric field affects only the internal motion and has no impact on the interlayer exciton's center-of-mass motion. Conversely, the out-of-plane electric field is expected to influence the center-of-mass energies due to the second term appearing in equation (**??**). To determine the out-of-plane electric field dependence of interlayer exciton center-of-mass energies, we solve the following center-of-mass Schrödinger equation:

$$\hat{H}_{CM}\Xi_{J,L}(R,\Phi) = E^{J,L}_{cm}(\Delta F_{\perp})\Xi_{J,L}(R,\Phi). \tag{5}$$

Here, $\hat{H}_{CM} = H_{CM} + V_s(R,\Phi)$, and $E^{J,L}_{cm}$ are the center-of-mass eigenvalues with the corresponding eigenvectors $\chi_{J,L}(R,\Phi) = \sum_{\tilde{J},\tilde{L}} A^{\tilde{J},\tilde{L}}_{J,L}(\Delta F_{\perp})\Xi_{J,L}(R,\Phi)$, where $A^{\tilde{J},\tilde{L}}_{J,L}(\Delta F_{\perp})$ represents the dominant coefficients of the eigenvectors obtained through the numerical diagonalization of equation (5). This investigation provides information on the center-of-mass energy shift and modifications to the center-of-mass orbital due to the effect of the out-of-plane electric field.

2 Photoluminescence and Moiré Exciton Lifetime

Once the electric field dependence of the moiré interlayer exciton energy spectra is determined by numerically diagonalizing the internal and center-of-mass Hamiltonians into their respective bases, we proceed to analyze the photoluminescence spectra and the radiative lifetime under varying electric field strengths. The one-photon photoluminescence (PL) spectra of moiré IX at low temperatures can be approximated to be proportional to the oscillator strength and calculated using the following formula[2,3]:

$$PL = f^{osc}_{n\ell,JL}\Theta(\hbar\omega_p - E^{IX}_{n\ell,JL}). \tag{6}$$

Here, $f^{osc}_{n\ell,JL}$ represents the oscillator strength, and its simplified expression is given by[2]:

$$f^{osc}_{n\ell,JL} = \frac{m_0}{m_e}\frac{E_g}{E^{IX}_{n\ell,JL}} \sum_{n'\ell',J'L'} D^{n\ell,JL}_{n'\ell',J'L'} |\phi_{n',\ell'}(r=0)|^2 \Big| \int \Xi_{J',L'}(R) d^2R \Big|^2. \tag{7}$$

With, $\Theta(\hbar\omega_p - E^{IX}_{n\ell,JL}) = \dfrac{\Gamma_0}{\pi((\hbar\omega_p - E^{IX}_{n\ell,JL})^2 + \Gamma_0^2}$ defines the energy conservation with respect to the state broadening Γ_0, where $\hbar\omega_p$ is the photon energy. Γ_0 defines the half width at half maximum of the IX line. $D^{n\ell,JL}_{n'\ell',J'L'}$ is the dominant coefficient of the eigenvectors obtained by numerical diagonalization of total Hamiltonian. $E^{IX}_{n\ell,JL} = E_g + E^{n\ell}_{JL}$ is the localized interlayer exciton energy, E_g is the heterobilayer band-gap energy and the IX total energy is approximated as $E^{n\ell}_{JL} = E_{n,\ell} + E^{J,L}_{cm}$. Furthermore, the radiative decay rate of the localized IX, as a function of the oscillator strength and moiré IX energy, is expressed as[2,3]:

$$\tau_{rad} = \frac{3m_0\hbar^2c^3}{4n_0e^2}\frac{1}{E^{IX}_{1s,00}f^{osc}_{1s,00}}. \tag{8}$$

Here, $n_0 = \sqrt{\varepsilon}$ denotes the effective optical refraction index of the environment, c is the speed of light and $E^{IX}_{1s,00}$ represents the moiré interlayer exciton ground state energy.

3 Additional results

Figures 1(a) and 1(b) illustrate the dependence of the interlayer exciton ground state Stark shift on the strength of the in-plane electric field across various values of the average dielectric environment ε and the spacing separation d, respectively. These results demonstrate

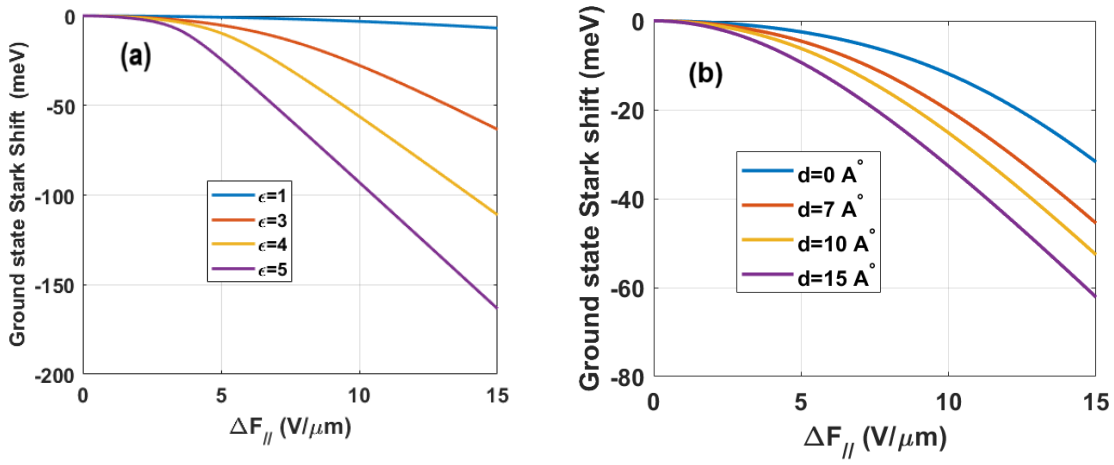

Fig. 1 Figures (a) and (b) depict the 1s ground state Stark shift of IX as a function of the in-plane electric field strength, considering various values of the effective dielectric environment ϵ and spacing separation d (A°) , respectively.

a considerable increase in the Stark shift when either ϵ or d is increased. It's important to note that as ϵ increases, the exciton's binding energy spectrum considerably decreases, leading to a less bound exciton. Consequently, the exciton becomes more susceptible to the electric field perturbation, as illustrated in figure 1(a). This assessment holds significant interest in optical materials modulation, wherein the spatial separation between the two layers can be controlled using hBN layers, a well-known technique.

References

1 D. A. Ruis-Tijerina, I. Soltero and F. Mirels. Theory of moiré localized excitons in transition metal dichalcogenide heterobilayers, Phys. Rev. B, 2020, **102**, 195403.

2 H E. Hannachi, D. Elmaghraoui and S. Jaziri. Moiré interlayer exciton relative and center of mass motions coupling. Effect on $1s-np$ interlayer exciton THz transitions, Eur. Phys. J. Plus, 2023, **138**, 396.

3 A. Smiri, T. Amand, and S. Jaziri. Optical properties of excitons in two-dimensional transition metal dichalcogenide nanobubbles, J. Chem. Phys, 2021, **154**, 084110.